JOURNAL OF MORPHOLOGY 245:206–224 (2000)

Morphometry of *Macaca mulatta* Forelimb. I. Shoulder and Elbow Muscles and Segment Inertial Parameters

Ernest J. Cheng[1] and Stephen H. Scott[2]*

[1]*Department of Physiology, Queen's University, Kingston, Ontario, Canada*
[2]*Department of Anatomy and Cell Biology, Queen's University, Kingston, Ontario, Canada*

ABSTRACT The present study examined the morphometric properties of the forelimb, including the inertial properties of the body segments and the morphometric parameters of 21 muscles spanning the shoulder and/or elbow joints of six *Macaca mulatta* and three *M. fascicularis*. Five muscle parameters are presented: optimal fascicle length (L_0^M), tendon slack length (L_S^T), physiological cross-sectional area (PCSA), pennation angle (α_0), and muscle mass (m). Linear regressions indicate that muscle mass, and to a lesser extent PCSA, correlated with total body weight. Segment mass, center-of-mass, and the moment of inertia of the upper arm, forearm, and hand are also presented. Our data indicate that for some segments, radius of gyration (ρ) predicts segment moment of inertia better than linear regressions based on total body weight. Key differences between the monkey and human forelimb are highlighted. J. Morphol. 245:206–224, 2000.

KEY WORDS: *Macaca mulatta*; shoulder; elbow; muscle morphometry; limb morphometry

Reaching movements by nonhuman primates (*Macaca mulatta*) have become a popular paradigm in which to study the involvement of different neural regions in motor planning and control (reviewed by Georgopoulos, 1995). Due to the complexities of these multijoint movements, neural discharge in various cortical and subcortical regions has usually been correlated to variables related to the hand, such as the direction of movement. While this approach minimizes the technical problem of quantifying the mechanics of multijoint motion, several studies have demonstrated that neural activity is not related simply to the hand, but also reflects features of movement related to the motor periphery (Fromm, 1983; Caminiti et al., 1990; Scott and Kalaska, 1997; Scott, 1997). Further progress on understanding cortical control of movement requires a better understanding of the physical properties of the monkey forelimb and how its muscles generate movement.

The laws of Newtonian motion dictate that muscular torque at a joint may cause motion at many joints in a multisegmented limb. To understand the relationship between muscle force and limb motion, biomechanical models have been used to study a variety of motor tasks in humans (e.g., Pierrynowski and Morrison, 1985; Zajac and Gordon, 1989; Seif-Naraghi and Winters, 1990; Kuo and Zajac, 1993) and in animals (e.g., Hoy and Zernicke, 1986; Dornay et al., 1993). These models are valuable not only for quantifying the mechanics of limb motion, but also for examining how the physical properties of the limb constrain control strategies used by the central nervous system to plan and execute movement.

Our long-term goal is to develop a musculoskeletal model of the monkey forelimb. Central to this project is the need for quantitative descriptions of the inertial properties of the limb segments, as well as the morphometric properties of muscles spanning the elbow and shoulder joints. The latter data are required by mathematical models of the force-generating capabilities of musculotendon systems, such as the commonly employed Hill-type model (Hill, 1938). Zajac (1989) described an implementation of this model using a "dimensionless" system of equations, where a generic musculotendon actuator could be scaled by five different muscle-specific parameters to estimate force production. The contractile element of the actuator requires four terms: L_0^M (optimal fascicle length, the length at which the muscle produces maximal tetanic isometric force), F_0^M (maximal tetanic isometric force), α_0 (pennation angle of the muscle fibers at L_0^M), and τ_C (time-scaling parameter for maximal muscle shortening velocity). The fifth term in the general muscle model

Contract grant sponsor: Medical Research Council of Canada; Contract grant number: MT-13462 (to S.H.S.). Contract grant sponsor: MRC Scholarship (to S.H.S.). Contract grant sponsor: Ontario Graduate Scholarship (to E.J.C.).

*Correspondence to: Stephen H. Scott, Department of Anatomy and Cell Biology, Queen's University, Kingston, Ontario, Canada K7L 3N6. E-mail: steve@biomed.queensu.ca

TABLE 1. Macaca mulatta; *general specimen morphometric data*

Animal	M3	M5	M6	M7	M9	M10	Mean
Sex	M	M	M	F	M	M	
Weight (kg)	4.6	6	9.8	4.4	10	12.4	7.9 ± 3.3
Shoulder to midline (cm)	4.7	5.5	6.5	5.2	6.5	6.7	5.9 ± 0.8
Upper arm length (cm)	13.5	14.5	16	11.6	15	15.7	14.4 ± 1.6
Forearm length (cm)	15	17	17.5	12.4	14	16.4	15.4 ± 2.0
Hand length (cm)	9.7	10.4	10.8	8.6	10	12.2	10.3 ± 1.2
Total arm length (cm)	38.2	41.9	44.3	32.6	39	44.3	40.1 ± 4.5

Mean values are ± standard error.

is the length of the series elastic element, L_S^T (tendon slack length).

Unfortunately, such data in monkeys are largely unavailable in the literature. Data on muscle masses for a number of proximal arm muscles have been recorded in two studies, but they only examined desiccated muscle mass (Dhall and Singh, 1977; Doyle et al., 1980). Dornay et al. (1993) identified parameters for many forelimb muscles, but only examined a single monkey, and did not provide the total body weight of the specimen. Roy et al. (1984) reported morphometric parameters from a larger sample of *Macaca fascicularis,* but only examined seven elbow muscles.

Inertial parameters of the limb segments are also required for developing musculoskeletal models. Vilensky (1978) provides measurements and linear regressions against total body weight that permit scaling of moments-of-inertia and segment masses in *Macaca mulatta*. The data of Vilensky are quite extensive, but his choice of total body weight as the independent regression variable differs from many existing procedures, which also account for segment length in their regressions (e.g., Forwood et al., 1985; Schneider and Zernicke, 1992). Another method for scaling moment-of-inertia is the use of segment radius of gyration (ρ); when scaled as a percentage of segment length (e.g., Jensen, 1986), this provides a dimensionless measure of moment of inertia. This value is determined such that an object with equal mass that is distributed as a point one radius of gyration away from the center of rotation would have the same rotational inertia.

This study provides a set of morphometric data for the muscles and skeletal segments of the *Macaca mulatta* arm and identifies correlations that can be used to scale these parameters to a given animal. A complete biomechanical model of the primate limb also requires measurements on the mechanical advantage of muscles about each joint and will be presented in a future study.

MATERIALS AND METHODS

General Specimen Information

Measurements of 21 muscles spanning the shoulder and elbow joints were made in five late juvenile and early adult male rhesus monkeys (*Macaca mulatta*) weighing 4.6–12.4 kg, and in one adult female monkey weighing 4.4 kg (Table 1). Although the focus of this study is to provide data for modeling the *M. mulatta* forelimb, similar data were also collected from three *M. fascicularis*. General specimen morphometric data for this species are presented in Table 2. The monkeys were cared for in accordance with Canadian Council on Animal Care Guidelines.

No monkeys were euthanized specifically for this study. In all cases, the monkeys were involved in neurophysiological studies and were euthanized for necessary histological analyses in those studies. While MR images have been used to identify morphometric properties of muscles in humans (i.e., Scott et al., 1993), these techniques cannot easily identify the anatomical organization of all muscles within a limb. Given the small size of monkeys, the need for a complete database and the availability of

TABLE 2. Macaca fascicularis; *general specimen morphometric data*

Animal	F1	F2	F4	Mean
Sex	M	F	M	
Weight (kg)	5.1	5.1	6.9	5.7 ± 1.0
Shoulder to midline (cm)	6	5.2	8	6.4 ± 1.4
Upper arm length (cm)	10.5	10.5	11	10.7 ± 0.3
Forearm length (cm)	13	13.2	13	12.9 ± 0.4
Hand length (cm)	8.3	7.6	9	8.3 ± 0.7
Total arm length (cm)	31.8	31.3	33	31.9 ± 0.6

Mean values are ± standard error.

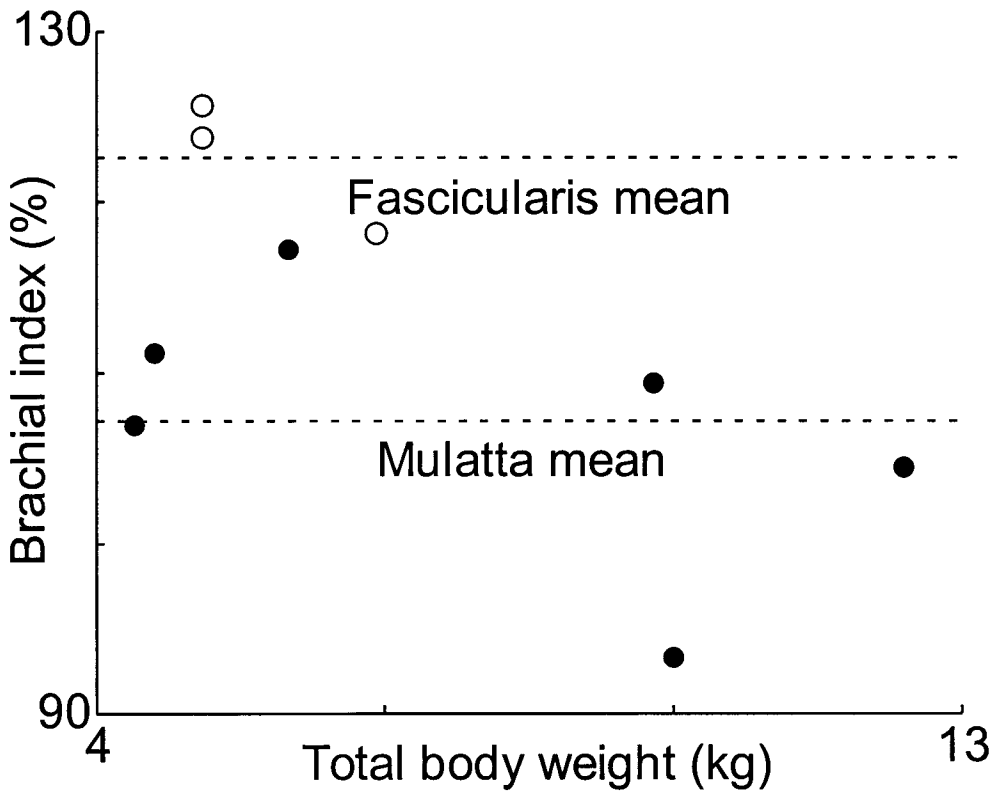

Fig. 1. Brachial index (%) versus body weight (kg) for *Macaca fascicularis* (○) (n = 3) and *M. mulatta* (●) (n = 6). Mean values are plotted as dotted lines.

cadaveric specimens, we decided to measure the muscle properties directly.

To obtain the necessary muscle and segment measurements, the animals were initially sedated with ketamine. The femoral artery was catheterized and the animals were anesthetized with sodium pentobarbital. The axis of rotation for each joint was determined by flexing and extending each segment and finding the point that remained motionless on rotation (Scott and Winter, 1991b). *Shoulder to midline* distance was measured as the distance from the center of rotation between the humerus and glenoid cavity of the scapula to the body midline (center of the manubrium). *Upper arm* length was measured from the center of rotation in the flexion–extension axis of the shoulder to the center of rotation of the elbow. *Forearm* length was measured as the distance from the center of rotation of the elbow to the center of rotation of the wrist. *Hand* length was measured along the face of the palm, from the wrist to the tip of the index finger.

Brachial index was calculated using the measurements for upper arm and forearm length to represent humerus and radial length, respectively. Napier (1967) defines *Brachial index* as follows:

$$\text{Brachial Index} = \frac{\text{Radius length} * 100}{\text{Humerus length}} \qquad (1)$$

Our measures differ slightly because we measured segments from joint center to joint center, while Napier measured bone lengths.

After measuring segment lengths, the animals were perfused intracardially with phosphate-buffered saline followed by a 10% formalin solution (Kalaska et al., 1989). During the perfusion, both arms were abducted approximately 90° from the anatomical position and held until fixation was completed. Muscle morphometry was measured from the right arm and segment inertial parameters were quantified from the left arm.

Muscle Morphometry

Zajac (1989) identified five muscle-specific terms required to predict force produced by a musculotendon element. Four of the five terms are examined in this study: optimal fascicle length (L_0^M), maximal tetanic isometric force (F_0^M), pennation angle (α_0), and tendon length (L_S^T). The velocity-related parameter τ_C is dependent on muscle histochemical fiber type and will be examined in a related article.

To determine a value for L_0^M, fascicle length of each muscle was measured by averaging lengths from three to five fascicles dissected in varying locations in the muscle. Superficial fascicles were generally avoided since they tend to be slightly longer

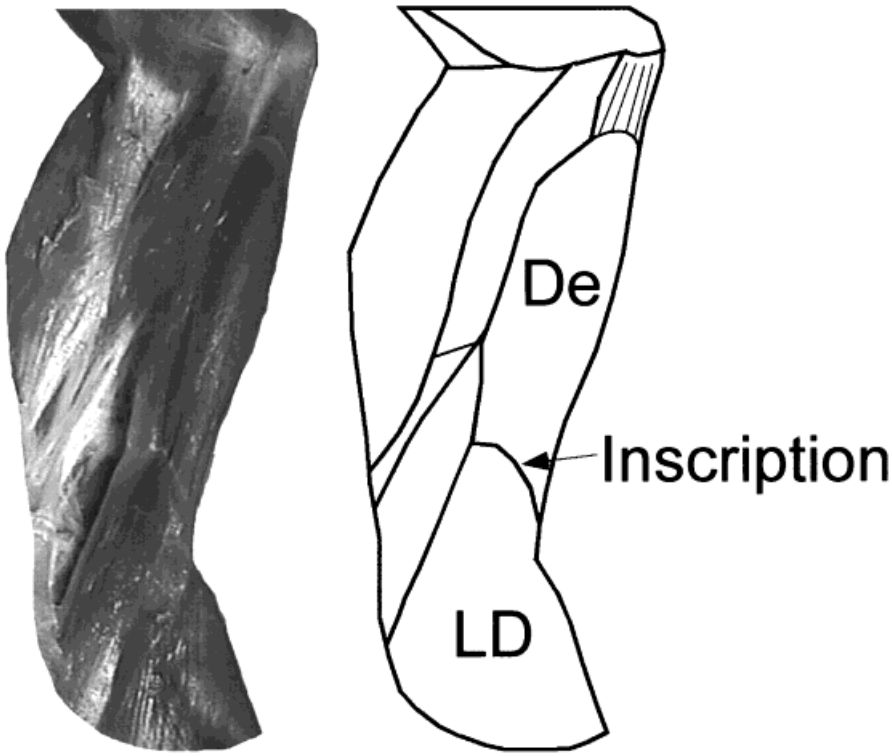

Fig. 2. *Macaca mulatta.* Medial view of left upper arm in a fully abducted posture. Dorsoepitrochlearis (De) is shown, attached to latissimus dorsi (LD) by a tendinous inscription.

than fascicles within the muscle belly (Kamibayashi and Richmond, 1998). Length shrinkage of muscle while being fixed in situ has been shown to be negligible (Cutts, 1988).

It was necessary to normalize the measurements to optimal fascicle length by examining the sarcomere lengths within each specific fixed muscle (Gordon et al., 1966; Scott et al., 1996). Excised fiber bundles from each measured fascicle were mounted on glass slides and cover-slipped with glycerol. Sarcomere lengths were measured typically from three to six random locations in each bundle and averaged

TABLE 3. Macaca mulatta; *shoulder and elbow muscle morphometry data (n = 6)*

Muscle	Abbreviation	L_0^M (cm)	Mass (g)	PCSA (cm^2)	L_0^T (cm)	α (°)
Biceps long	BL	5.4 ± 0.6	27.1 ± 11.7	4.6 ± 1.7	8.8 ± 1.7	7 ± 2
Biceps short	BS	6.6 ± 1.1	17.5 ± 7.2	2.6 ± 1.2	5.7 ± 2.8	—
Brachialis	B	4.3 ± 0.8	16.75 ± 6.7	3.7 ± 1.2	2.9 ± 1.3	—
Brachioradialis	Br	11.1 ± 1.5	21.3 ± 10.0	1.7 ± 0.7	3.6 ± 1.8	—
Coracobrachialis	Cb	1.8 ± 0.7	2.5 ± 0.9	1.4 ± 0.2	5.1 ± 0.9	13 ± 12
Deltoid anterior	DA	5.2 ± 1.1	11.1 ± 4.4	1.9 ± 0.5	0.3 ± 0.5	—
Deltoid middle	DM	2.7 ± 0.4	14.7 ± 6.2	5.2 ± 2.1	1.9 ± 0.6	20 ± 9
Deltoid posterior	DP	4.7 ± 0.6	10.2 ± 5.1	2.0 ± 0.8	1.5 ± 0.8	—
Dorsoepitrochlearis	De	5.8 ± 1.0	9.1 ± 4.5	1.4 ± 0.6	4.4 ± 1.2	—
Extensor carpi radialis brevis	ECRB	3.1 ± 0.9	8.6 ± 3.7	2.8 ± 1.3	10.1 ± 1.6	—
Extensor carpi radialis longus	ECRL	5.7 ± 1.0	9.5 ± 5.9	1.5 ± 1.1	10.0 ± 1.9	—
Infraspinatus	Is	2.5 ± 0.5	22.0 ± 11.1	8.6 ± 4.5	4.0 ± 1.3	15 ± 8
Latissimus dorsi	LD	11.5 ± 2.2	57.1 ± 24.8	4.7 ± 2.0	11.3 ± 2.1	—
Pectoralis major	PM	7.9 ± 1.5	65.4 ± 29.0	7.6 ± 2.0	0.7 ± 0.5	—
Subscapularis	Sb	1.9 ± 0.3	32.0 ± 14.0	15.8 ± 5.6	4.1 ± 1.4	22 ± 3
Supraspinatus	Sp	2.6 ± 0.4	18.5 ± 5.3	6.9 ± 2.2	2.4 ± 1.2	15 ± 5
Teres major	TMa	5.7 ± 0.6	22.2 ± 8.5	3.7 ± 1.2	2.7 ± 0.7	14 ± 12
Teres minor	TMi	1.8 ± 0.4	2.9 ± 1.3	1.5 ± 0.5	1.4 ± 1.0	12 ± 7
Triceps lateral	TLa	4.3 ± 0.6	36.7 ± 15.9	7.7 ± 2.4	9.3 ± 1.2	21 ± 2
Triceps long	TLo	3.8 ± 0.5	41.9 ± 18.3	10.4 ± 4.8	9.5 ± 1.3	31 ± 8
Triceps medial	TMe	4.2 ± 0.4	20.0 ± 5.9	4.4 ± 1.2	3.2 ± 1.9	18 ± 7

Mean values are ± standard errors.

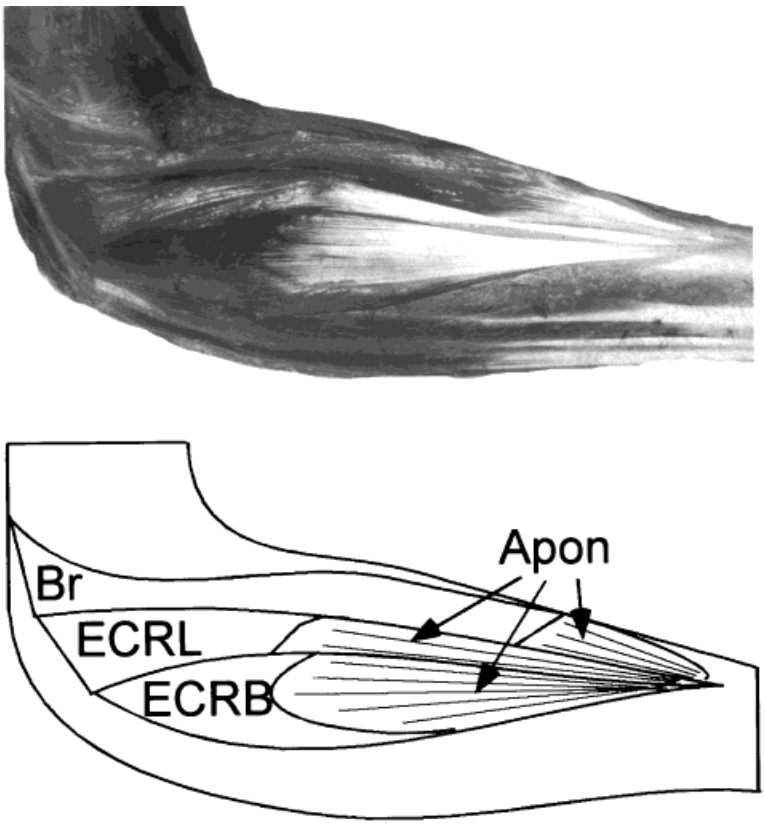

Fig. 3. *Macaca mulatta*. Medial view of right forearm at 90° flexion, depicting brachioradialis (Br), extensor carpi radialis longus (ECRL) and -brevis (ECRB). These muscles have been retracted to expose their aponeuroses. The aponeuroses of ECRL and ECRB normally face each other. Note that despite similar whole muscle path lengths, ECRL and ECRB have longer aponeuroses and shorter fascicles than Br.

for each fascicle. Each fascicle length for the muscle was then corrected to match the optimal *Macaca mulatta* sarcomere length of 2.41 μm (Walker and Schrodt, 1974). This is the minimum sarcomere length at which isometric tetanic force becomes maximal, as thin and thick filament overlap is maximized (Gordon et al., 1966). The individual fascicle lengths were averaged together within each muscle to obtain a mean L_0^M.

The maximal isometric force for a given muscle, F_0^M, is proportional to its physiological cross-sectional area (PCSA). F_0^M is calculated by multiplying PCSA for any muscle by peak stress, which appears to be constant for many mammalian muscle fiber types (Spector et al., 1980; Lucas et al., 1987). Alexander and Vernon's (1975) calculation for PCSA was used:

$$\text{PCSA} = \frac{m}{\rho \times L_0} \qquad (2)$$

where m = muscle mass (g), ρ = muscle density, 1.06 (g/cm^3) (Mendez and Keys, 1960), and L_0 = optimal fascicle length (cm). While it is common to include the cosine of the pennation angle in the numerator for this term (e.g., Bodine et al., 1982), this term is treated separately in the model described by Zajac. The cosine term acts to capture only the component of the force acting in the direction of the principle line of action for the muscle. By including this term in the PCSA, the pennation angle is treated as fixed for the entire range of muscle movement, an inaccurate assumption; pennation angle typically increases as a muscle contracts and shortens (Gans and Bock, 1965). A more accurate method would be to use a dynamic pennation angle, or even to neglect it altogether (Scott and Winter, 1991a).

Muscle mass was measured after excising any tendon and excess fat and fascia. Because muscles tend to dehydrate after dissection, mass was measured as soon as possible after each muscle was excised. As mentioned above, this mass is required for calculating PCSA, and thus F_0^M. Mass was adjusted to compensate for the 7% decrease in weight after fixation in formaldehyde (Schremmer, 1967).

Slack length of the connective tissue element, L_S^T, is also required for Zajac's musculotendon model. Length of tendons and aponeuroses at both origin and insertion were measured in each muscle. It is important to include all of the connective tissue between the contractile elements (the fascicles) and their targets (the bony origin and insertion). Accordingly, care was taken to dissect and measure the full length of the internal tendons within the muscle

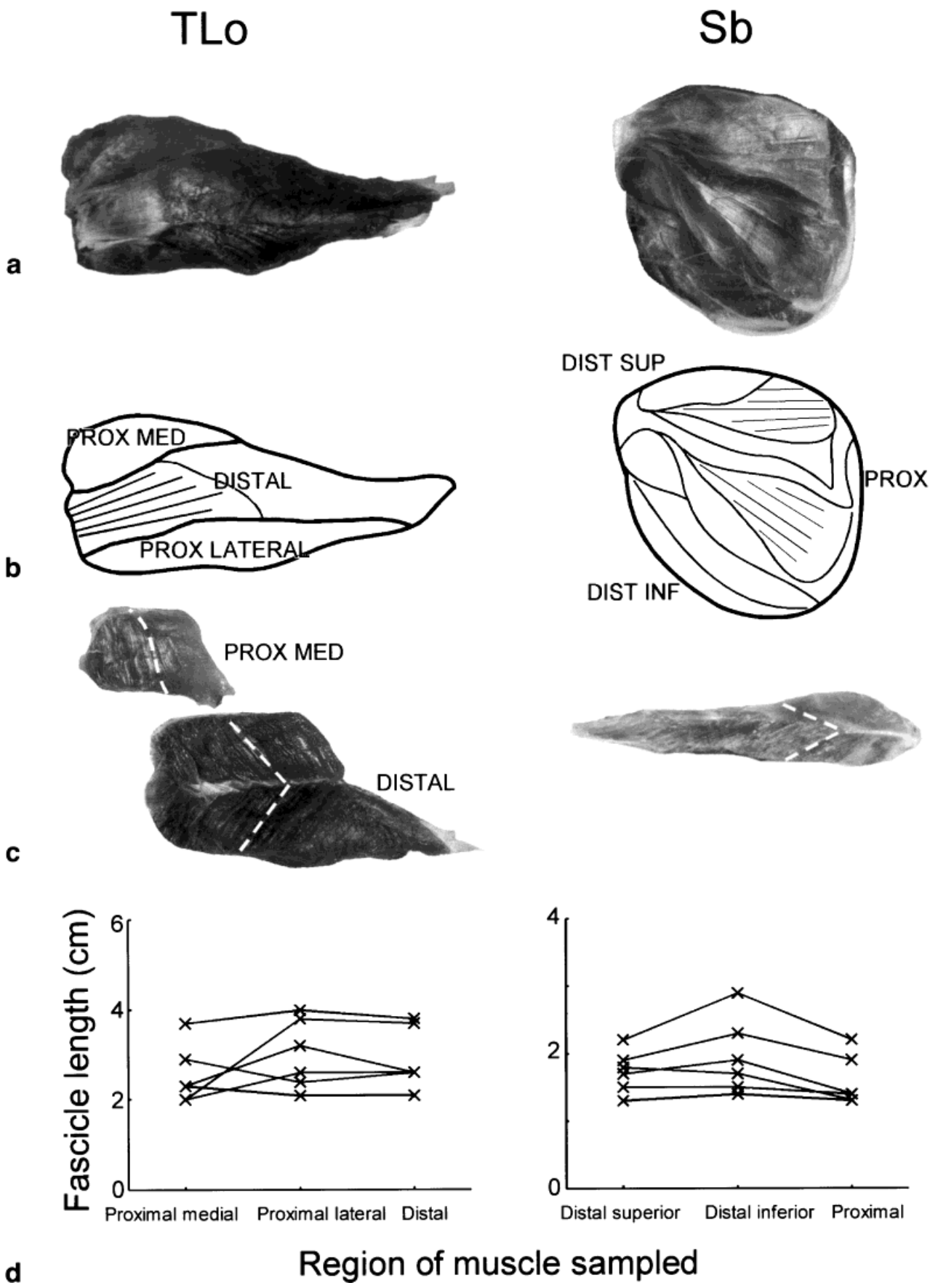

Fig. 4. *Macaca mulatta*. **a,b**: Views of superficial aspect of triceps long head (TLo) on left and subscapularis (Sb) on right. TLo consists of three differently shaped portions, while subscapularisis has numerous compartments joined by a complex network of aponeuroses. **c**: Cross-sections reveal that fascicle lengths (indicated by dotted lines) remain consistent despite complex muscle architecture. **d**: Plot of fascicle lengths (cm) in different regions from six animals. Note that fascicle lengths do not show any systematic variation based on their location in the muscle.

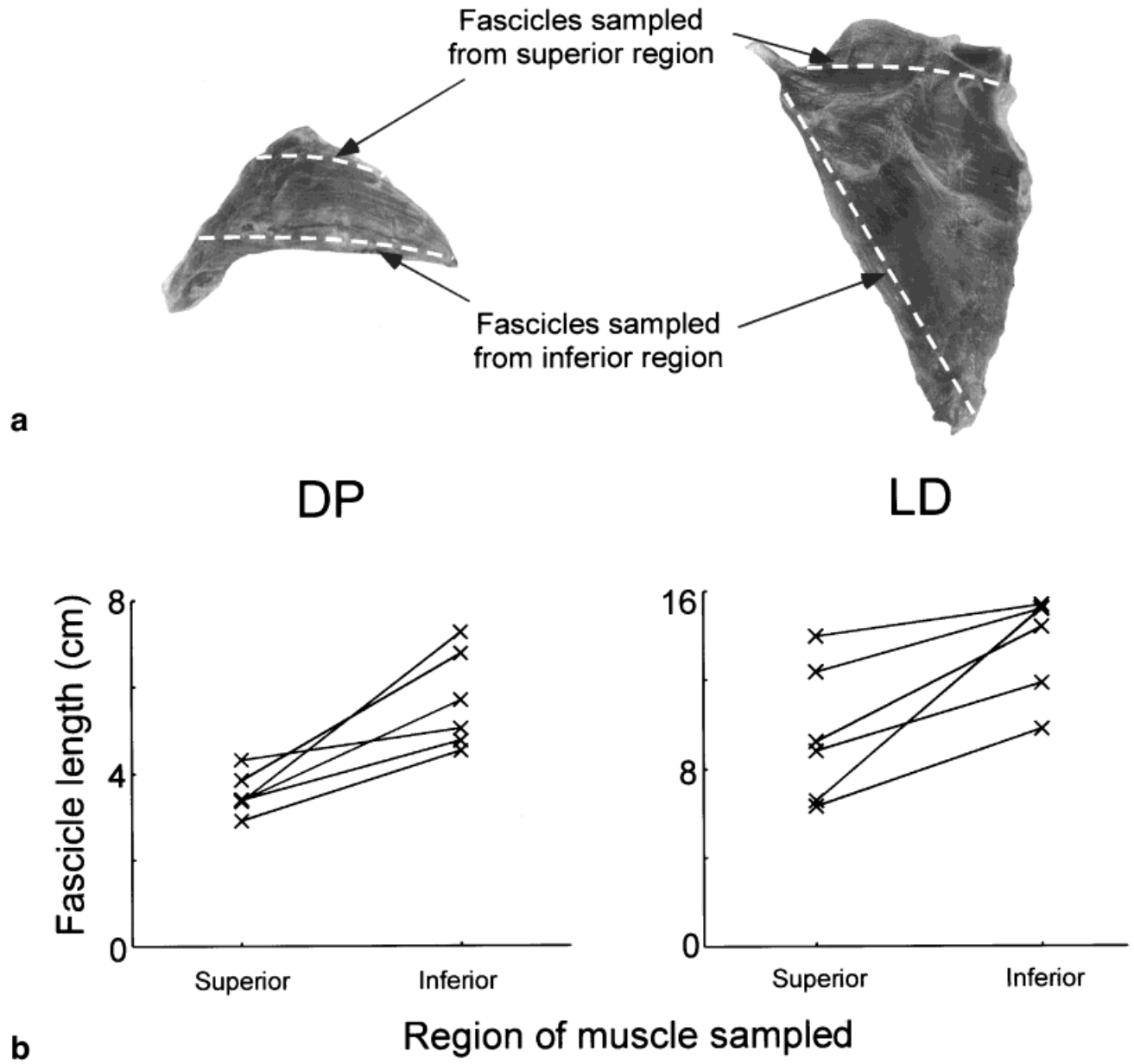

Fig. 5. *Macaca mulatta*. **a**: Views of posterior deltoid (DP) from the right forelimb and latissimus dorsi (LD), depicting two regions where fascicle lengths were sampled (indicated by dotted lines). **b**: Fascicle lengths (cm) in different regions of both muscles are plotted. Note the longer fascicles at the inferior parts of the muscle, which are farther from the axis of rotation of the shoulder joint.

belly. It has been shown that tendon and aponeurosis in cat soleus have similar mechanical properties (Scott and Loeb, 1995). It was assumed that each "average" fascicle was in series with the entire length of tendon, and half of the aponeurosis and internal tendon length, as given below:

$$L_S^T = \tfrac{1}{2}(L_{Org}^A + L_{Ins}^A) + (L_{Org}^T + L_{Ins}^T) \qquad (3)$$

where $L_{Org}{}^A$ and $L_{Ins}{}^A$ represent the aponeurosis and internal tendon lengths and $L_{Org}{}^T$ and $L_{Ins}{}^T$ the external tendon lengths at the origin and insertion, respectively. In some muscles, a portion of the fascicles insert or originate on a tendon or aponeurosis, while the remaining fascicles insert or originate directly from bone. In these cases, an estimate of the percentage of fascicles actually inserting onto tendon or aponeurosis was used to scale the relevant term in Eq. 3. For example, if only 50% of a given muscle originated from a 4 cm tendon, then $L_{Org}{}^T$ would be calculated as 2 cm.

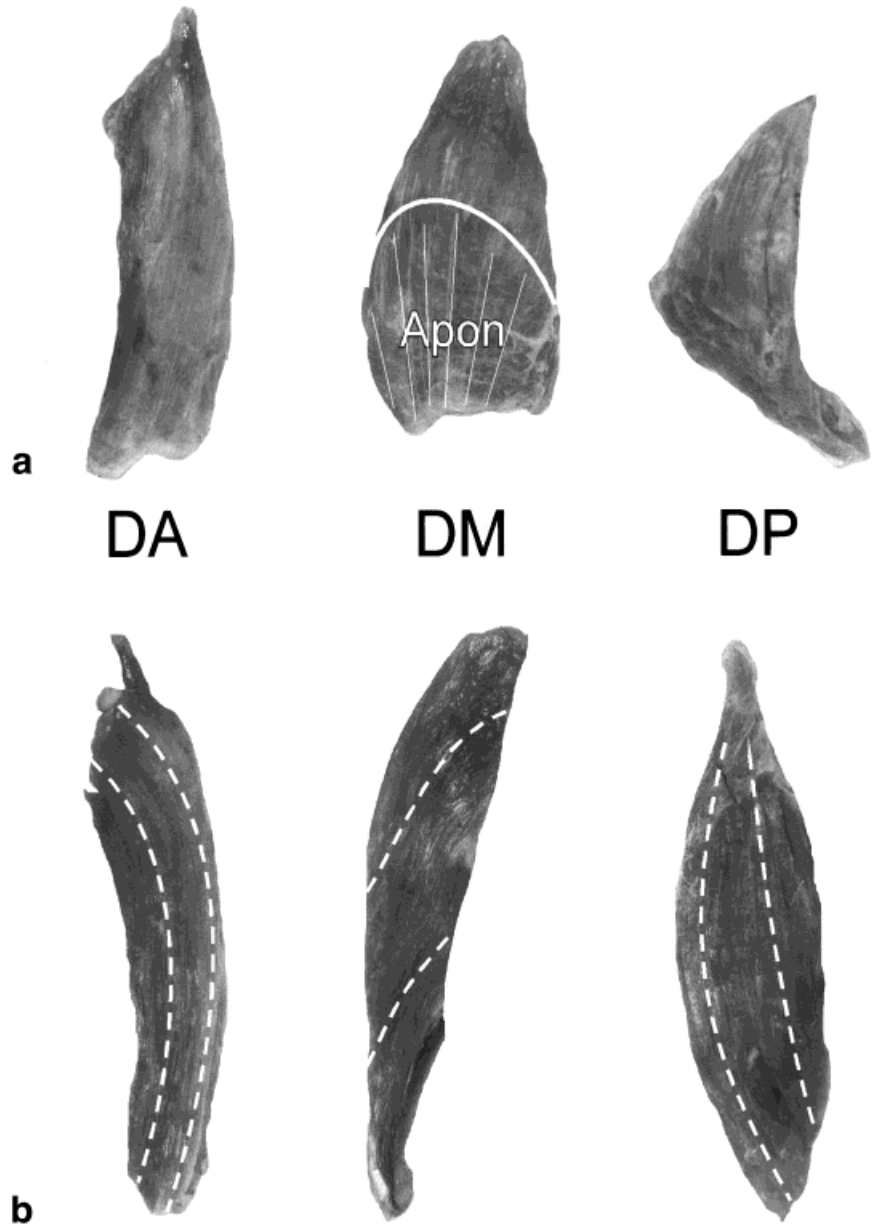

Fig. 6. *Macaca mulatta*. **a**: Views of the superficial aspect of anterior (DA), middle (DM), and posterior deltoid (DP). Note the large aponeurosis (Apon) present in DM only. **b**: Cross-sections reveal that because of the aponeurosis, fascicles (indicated by dotted lines) do not run the entire muscle belly length in DM, unlike DA and DP.

Pennation angle (α_0), defined as the angle between the direction of the muscle fibers and the principal line of action for that muscle (Gans and Bock, 1965), was measured using a protractor. In pennate muscle, it was averaged from three to six sites within the muscle. Investigators (e.g., Zajac, 1989; Scott and Winter, 1991a; Veeger et al., 1997) have suggested that pennation angle could be neglected for muscles that were not highly pennate. In this study, all angles below 5° were considered negligible, and thus ignored.

To determine whether the morphometric parameters (L_0^M, muscle mass, PCSA, L_S^T and α) could be extrapolated to animals of different sizes, linear regressions with both slope and Y-intercept terms were used. As independent variables, total body weight and each of the segment length measures were used. In the case of PCSA, which is expressed in units of length squared, total body weight$^{2/3}$ was used as an independent variable, and for L_0^M and L_S^T, total body weight$^{1/3}$ was used.

TABLE 4. Macaca mulatta; *linear regressions for muscle mass (g) and PCSA (cm^2) against total body weight (kg)*

	Muscle mass (g)			PCSA (cm^2)		
Muscle	m (slope)	b (Y-intercept)	*P*	m (slope)	b (Y-intercept)	*P*
Biceps long	3.32	0.85	*	0.44	1.14	*
Biceps short	1.89	2.55	*	0.17	1.14	
Brachialis	1.99	1.00	*	0.29	1.34	*
Brachioradialis	2.94	−2.02	*	0.17	0.30	*
Coracobrachialis	0.18	1.09		0.00	1.41	
Deltoid anterior	1.30	0.86	*	0.12	0.99	
Deltoid middle	1.83	0.32	*	0.54	0.83	*
Deltoid posterior	1.44	−1.11	*	0.23	0.15	*
Dorsoepitrochlearis	1.17	−0.14	*	0.16	0.17	*
ECRB	0.77	2.41		0.23	−0.27	
ECRL	1.53	−2.67	*	0.09	2.05	
Infraspinatus	2.92	−0.96	*	1.02	0.54	
Latissimus dorsi	7.10	1.15	*	0.49	0.72	*
Pectoralis major	8.51	−1.49	*	0.61	2.73	*
Subscapularis	4.16	−0.78	*	1.58	3.31	*
Supraspinatus	1.40	7.48	*	0.35	4.06	
Teres major	2.18	4.89	*	0.33	1.00	*
Teres minor	0.37	−0.03	*	0.15	0.28	*
Triceps lateral	4.72	−0.57	*	0.68	2.34	*
Triceps long	5.26	0.55	*	1.10	1.73	
Triceps medial	1.57	7.65	*	0.25	2.51	

Values for m (slope) and b (Y-intercept) are given. Significance ($P < 0.05$) is indicated by an asterisk (*) in the *P* column.

Limb Segment Inertial Properties

The inertial properties of the arm, including length, mass, location of center of mass, and moment of inertia, are needed to calculate joint kinetics using inverse dynamic models (e.g., Hollerbach and Flash, 1982; Hoy et al., 1990; Karst and Hasan, 1991; Scott, 1999). To obtain these measurements, the perfused left limb was disarticulated at the shoulder joint and frozen at -4°C. Weight of the limb changed by less than 1% on average after being frozen. The limb was cut at the elbow and wrist to produce upper arm, forearm, and hand segments whose weights were measured. The arm had been frozen in a straightened position to facilitate making cuts orthogonal to the long axis of the segment, with each section cut 1 cm thick. The thickness of each section was measured after cutting, corrected for blade thickness, and weighed.

Distance of the center of mass for each segment from the proximal joint center was determined using:

$$x = \frac{m_1x_1 + m_2x_2 + \ \ldots\ + m_nx_n}{m_1 + m_2 + \ \ldots\ + m_n} \qquad (4)$$

where x = distance of center of mass from proximal joint center (cm), m_i = mass of i^{th} section (g), and x_i = distance from proximal center of rotation of i^{th} section (cm) (Winter, 1979). The location of the center of mass was expressed as a percentage of that segment's length from the proximal joint center (e.g., Vilensky, 1978).

The moment of inertia of the segment about both the center of mass (I_{cg}) and the center of rotation of the proximal joint (I_{prox}) were determined by summing the inertia of each slice about the axis of rotation, as described by Winter (1979):

$$I = m_1x_1^2 + m_2x_2^2 + \ \ldots\ + m_nx_n^2 = \sum_{i=1}^{n} m_ix_i^2 \qquad (5)$$

where I = moment of inertia about a given center of rotation ($g \cdot cm^2$), m_i = mass of the i^{th} section (g), x_i = distance from axis of rotation of i^{th} section (cm).

The radius of gyration of the segment was calculated and normalized to segment length (e.g., Jensen, 1986). This term is defined as the distance at which a point mass equal to the original body would have to be placed to have the same moment of inertia, and can be calculated using the following equation (Winter, 1979):

$$I_{cg} = m\rho^2 \qquad (6)$$

where ρ = radius of gyration in cm.

Linear regression of segment mass against total body weight and I_{cg} against total body weight were also performed. Regression techniques were identical to those described for the muscle morphometry.

To determine the best method of summarizing moment of inertia for each segment across different individuals, the use of a single radius of gyration

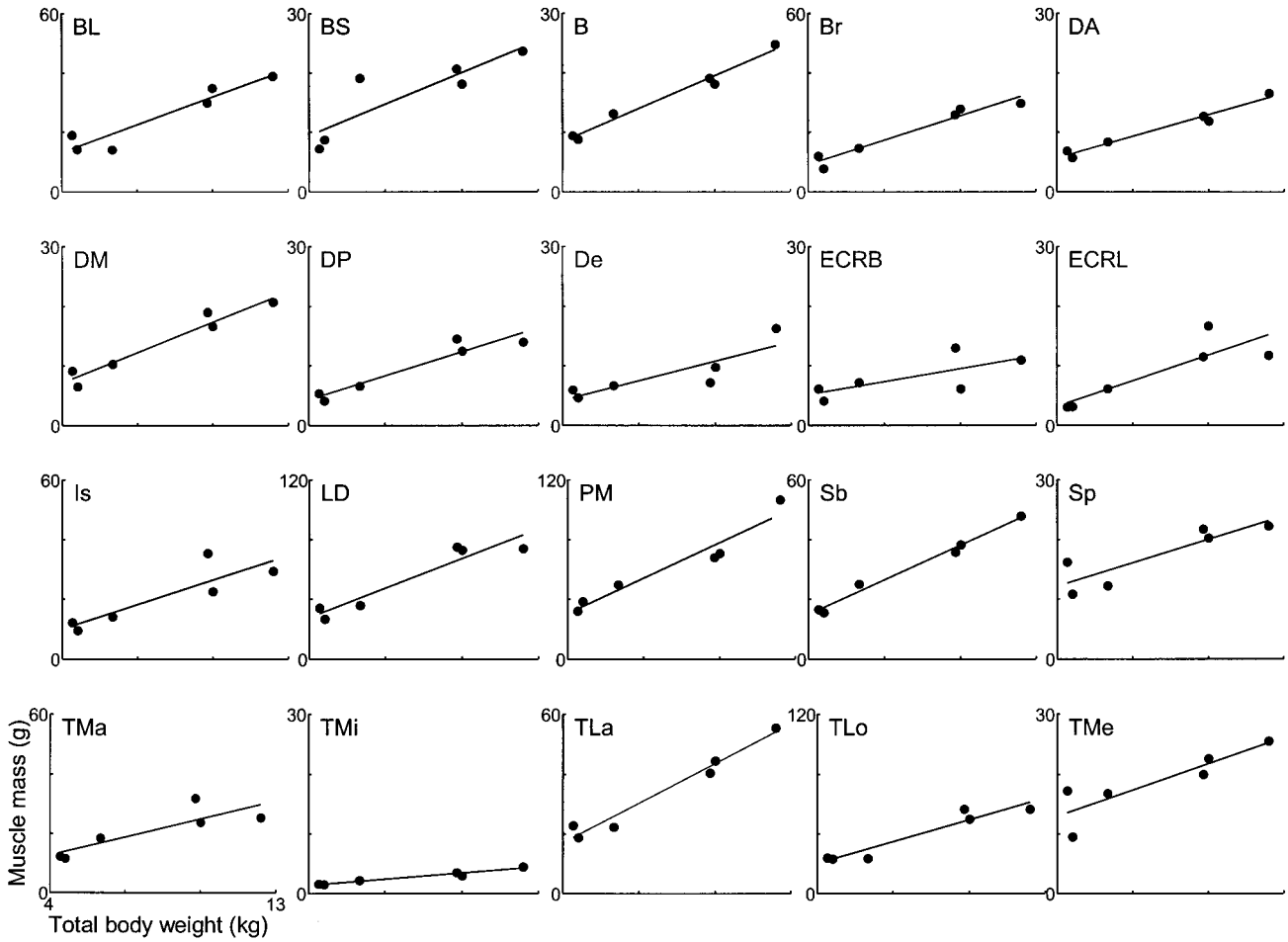

Fig. 7. Regressions of muscle mass (g) vs. total body weight (kg) for forelimb muscles in six *Macaca mulatta*. Measured data are indicated by filled circles, while linear fit regressions are indicated by straight lines.

value was compared to a linear regression of I_{cg} against total body weight. In the former case, I_{cg} was predicted for each specimen using the mean ρ of all specimens and parameters that could be measured in an intact monkey:

$$I_{\text{cg predicted}} = m_{\text{predicted}} \times \left(\frac{\rho_{\text{average}}}{100} \times l_{\text{measured}} \right)^2 \quad (7)$$

where $m_{\text{predicted}}$ = segment mass predicted using the linear regression against the animal's total body weight, ρ_{average} = the mean radius of gyration from our data as a percentage of segment length, and l_{measured} = segment length measured from the specimen.

RESULTS

While heavier animals tended to have longer segment lengths, the variation of the length measures was much less than that of total body weight. For *Macaca mulatta*, standard deviations for segment length measures were only 12% of mean values, while the corresponding coefficient of variation for total body weight was 42%. For *M. fascicularis*, coefficient of variation was 8% for length measures and 17% for total body weight.

In general, *Macaca fascicularis* specimens were lighter, had much shorter upper arms, but had broader shoulders. The proportional difference in segment lengths is reflected in the brachial index (Fig. 1), with a mean of 108 for *M. mulatta* and 121 for *M. fascicularis* ($P < 0.05$, Student's *t*-test). Brachial index did not show a significant variation with total body weight for either species, which suggests that size differences alone do not account for the variation in brachial indices.

Muscle Morphometry

Based on observation of origins and insertions during dissection, actions of most monkey forelimb

TABLE 5. Macaca fascicularis; *shoulder and elbow muscle morphometry data (n = 1–3)*

Muscle	n	L_0^M (cm)	Mass (g)	PCSA (cm^2)	L_0^T (cm)	α (°)
Biceps long	3	4.6 ± 0.6	20.3 ± 4.8	4.3 ± 1.6	7.9 ± 0.5	11 ± 5
Biceps short	3	6.5 ± 1.7	7.6 ± 3.4	1.3 ± 1.0	5.3 ± 1.4	—
Brachialis	2	4.4 ± 1.6	9.1 ± 3.0	2.2 ± 1.4	2.1 ± 0.1	—
Brachioradialis	2	8.5 ± 3.2	14.4 ± 6.2	1.8 ± 1.4	2.8 ± 0.5	—
Coracobrachialis	3	1.1 ± 0.2	1.8 ± 0.2	1.6 ± 0.1	3.6 ± 2.1	13 ± 12
Deltoid, anterior	3	5.1 ± 0.4	7.6 ± 2.1	1.5 ± 0.5	0.1 ± 0.2	—
Deltoid, middle	3	2.6 ± 0.1	10.3 ± 2.0	3.8 ± 0.9	1.9 ± 0.1	22 ± 3
Deltoid, posterior	3	4.4 ± 0.7	5.1 ± 1.8	1.1 ± 0.4	1.3 ± 0.3	—
Dorsoepitrochlearis	2	5.5 ± 0.7	7.3 ± 2.5	1.3 ± 0.5	3.0 ± 0.1	—
Extensor carpi radialis brevis	1	2.7	5.4	2.4	10.0	12
Extensor carpi radialis longus	1	4.7	18.3	4.1	7.9	—
Infraspinatus	2	2.4 ± 0.3	15.0 ± 3.4	6.1 ± 2.0	4.6 ± 1.4	8 ± 11
Latissimus dorsi	2	10.6 ± 1.6	48.1 ± 22.5	4.2 ± 1.4	7.8 ± 0.6	—
Pectoralis major	3	6.8 ± 1.6	37.2 ± 1.3	5.3 ± 1.5	0.8 ± 0.4	—
Subscapularis	2	1.8 ± 0.3	24.1 ± 10.5	12.8 ± 7.3	2.9 ± 0.9	24 ± 11
Supraspinatus	3	2.9 ± 0.2	11.3 ± 3.0	3.7 ± 0.7	3.6 ± 0.5	8 ± 7
Teres major	2	4.5 ± 0.2	14.7 ± 5.1	3.1 ± 1.0	3.3 ± 1.5	16 ± 6
Teres minor	1	1.3	2.5	1.8	1.4	10
Triceps lateral	2	3.6 ± 0.9	25.5 ± 3.8	7.1 ± 2.7	7.0 ± 1.7	27 ± 8
Triceps long	2	3.9 ± 0.4	33.2 ± 10.0	8.1 ± 1.6	6.6 ± 0.4	29 ± 1
Triceps medial	2	3.9 ± 1.6	12.4 ± 0.2	3.3 ± 1.4	2.9 ± 1.0	26 ± 2

Mean values are ± standard errors.

muscles parallel that of their counterparts in humans. The most notable difference between the two species is the dorsoepitrochlearis muscle, which does not exist in most humans but is present in all monkeys (Howell and Straus, 1961). This muscle originates directly from a tendinous inscription into the muscle belly of latissimus dorsi in the axillary region and inserts partly into the superficial olecranon fascia of the ulna and partly to the medial epicondyle of the humerus (Fig. 2). Functionally, it acts to extend the elbow and adduct the upper arm. Dorsoepictrochlearis has been described as an extension of the triceps complex (Howell and Straus, 1961), and has been labeled as a "climbing muscle" (Sonntag, 1922).

The optimal fascicle length (L_0^M), mass, PCSA, connective tissue length (L_S^T) and pennation angle (α_0) for the 21 *Macaca mulatta* muscles measured in this study are listed in Table 3. The sole female *M. mulatta* in the study was also the smallest. Aside from its size, inspection of the regression data for muscle mass and PCSA did not reveal any striking disparity with the other male monkeys.

Optimal fascicle length data is given in the first column of the table. Standard deviations of this term between monkeys were the lowest out of the listed terms, on average 17% of mean length. Latissimus dorsi had the longest fascicles and also the greatest length of tendon. Second in fascicle length at 11.1 cm was brachioradialis, which originates from the distal end of the humerus and runs along the forearm, inserting at the distal end of the radius. Interestingly, the two muscles immediately deep to brachioradialis are extensor carpi radialis longus (ECRL) and brevis (ECRB), which have similar total path lengths to brachioradialis, but have fascicle lengths which are much shorter: 5.7 and 3.1 cm, respectively (Fig. 3). These latter two muscles also had, aside from latissimus dorsi, the greatest tendon slack length at approximately 10 cm. Examination of these three muscles in situ reveals that the ECRL and ECRB both have much longer aponeuroses than brachioradialis, which accounts for these muscle morphometry differences.

The muscle with the greatest angle of pennation was the triceps long head. This muscle consists of several irregularly shaped portions; a thick proximal medial portion, a long and flat distal portion, and a medium-sized lateral portion (Fig. 4). All fascicles insert on a broad sheet of aponeurosis. Despite the complex architecture, fascicles in different parts of the muscle remained similar in length. Similarly complex in architecture is the subscapularis muscle, which originates from the medial surface of the scapula and inserts on the lesser tuberosity of the humerus (Howell and Straus, 1961). Subscapularis has a network of internal tendons that provide origin and insertion points for a large number of relatively short fascicles. The muscle has the appearance of being composed of numerous, separate compartments, each originating from or inserting on a different plane of aponeurosis. Again, despite the complex organization of the muscle, fascicle length is conserved throughout the different compartments of the muscle (Fig. 4).

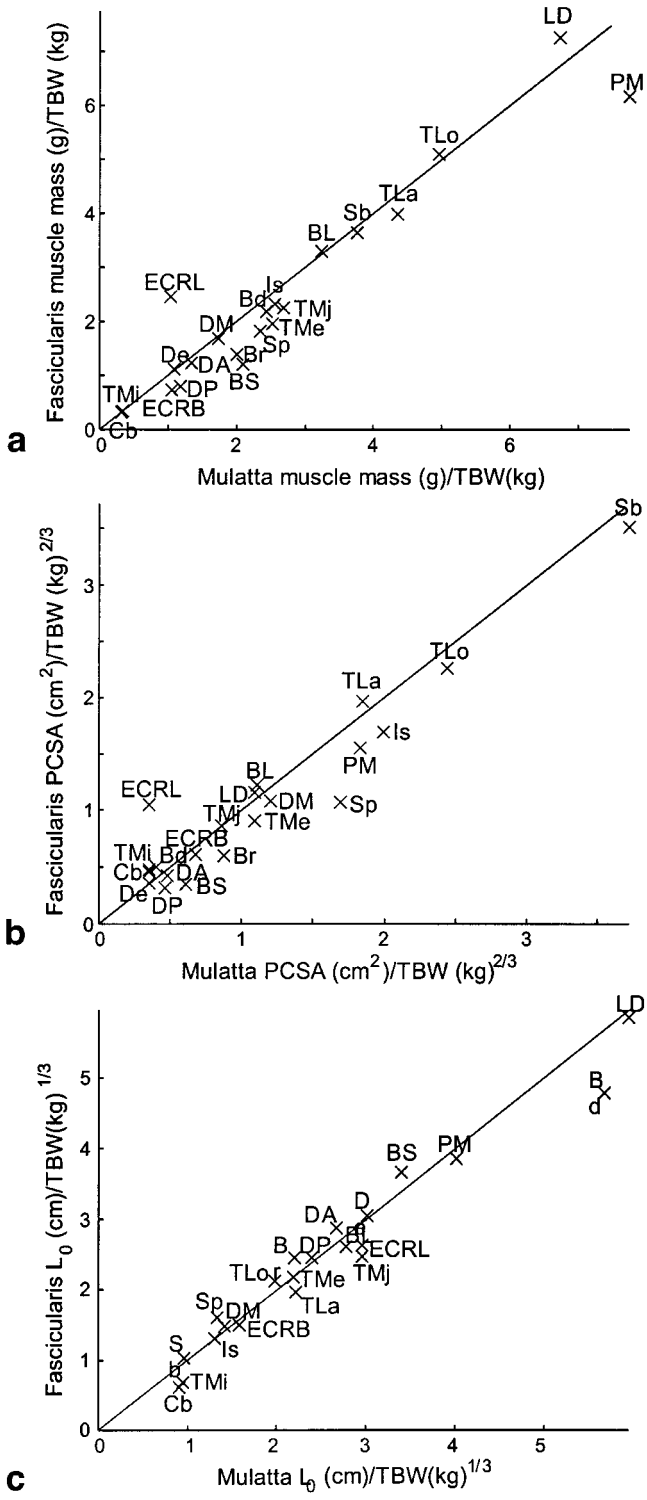

Fig. 8. Comparison of scaled mean muscle measures in *Macaca fascicularis* (n = 6) vs. *Macaca mulatta* (n = 3). **a**: Muscle mass (g) scaled by total body weight (kg), **b**: physiological cross-sectional area (cm^2) scaled by total body weight$^{2/3}$, and **c**: fascicle length (cm) scaled by total body weight.$^{1/3}$.

On the other hand, some muscles had no pennation angle and seemingly simple architectures, which disguise a sophisticated organization of varying fascicle lengths. For example, the posterior deltoid (Fig. 5a) consists of fibers that originate from an aponeurosis at the crest of the scapula and insert into the deltoid crest of the humerus. However, fascicle lengths varied systematically, with shorter fascicles near the superior region of the muscle, increasing in length as we move towards the inferior region of the muscle (Fig. 5b). Functionally, the effect is that the shorter fascicles near the axis of rotation have a reduced absolute change in length with any change in joint angle, compared to the more inferior part of the muscle. Thus, fascicles both proximal and distal to the axis of rotation have a similar proportional length change. This orderly arrangement of varying fascicle lengths was also observed in the latissimus dorsi. Latissimus dorsi is a triangular, flat sheet of muscle which had shorter fascicles at its superior region, closer to the axis of rotation for the shoulder (Fig. 5).

Musculotendon path lengths and muscle belly lengths were not good indications of fascicle length. For example, the three parts of the deltoid lie adjacent to one another and have similar total path lengths, as depicted in *Macaca mulatta* in Figure 6. However, a sheet of aponeurosis at the origin of the middle deltoid provides a greater surface area for fascicles to originate from, allowing a greater cross-sectional area. The fascicles have a significant angle of pennation, while the neighboring anterior and posterior deltoid have no angle of pennation. Consequently, the middle deltoid sacrifices fascicle length for an enhanced cross-sectional area. This architecture differs from that in humans, where the middle deltoid lacks an aponeurosis at the origin.

As compared to other muscle variables, muscle mass varied the most. Standard deviations were on average 43% of the mean values. Described previously, the greater variation of mass values can be explained allometrically; mass is proportional to volume, which varies with the cube of linear measures. Units of PCSA vary with the square of length measures, and units of $L_0{}^M$ and $L_0{}^T$ are directly proportional to length. These differences in the variation of the muscle measures parallels the differences in variation of the overall monkey morphometry measures, since total body weight varied much more than segment lengths. The muscle with the largest PCSA and consequently capable of producing the most force is subscapularis, with a PCSA of 15.8 cm^2. This cross-sectional area is more than double that observed for the much heavier pectoralis major muscle. Subscapularis' large PCSA is a consequence of its very short mean fascicle length of 1.9 cm and a moderate mass. The network of internal tendons, described previously, facilitates the short fascicle

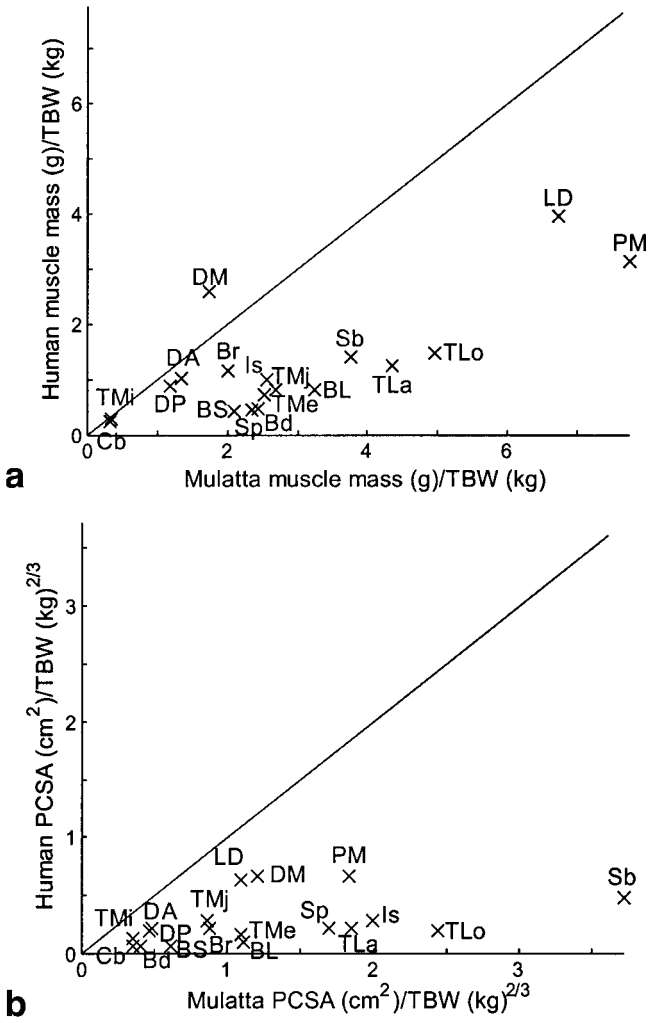

Fig. 9. Comparison of scaled mean muscle measures in human (from Veeger et al., 1997) vs. *Macaca mulatta* (n = 6). **a**: Muscle mass (g) scaled by total body weight (kg). **b**: Physiological cross-sectional area (cm^2) scaled by total body weight$^{2/3}$. Human data lacked fascicle lengths, so no comparison could be made.

lengths. The three muscles with the greatest PCSA all had pennation angles over 15°.

Significant regressions were found for a majority of *Macaca mulatta* forelimb muscles for muscle mass against total body weight, and PCSA against total body weight$^{2/3}$, listed in Table 4. Figure 7 illustrates data for regressions of muscle mass against total body weight, excluding coracobrachialis, which did not show a significant correlation. The regression of PCSA against total body weight$^{2/3}$ produced similar significance levels to regression against total body weight; total body weight$^{2/3}$ was chosen because it generally yielded a lower y-intercept term. Regressions of $L_0{}^M$, α_0, and $L_S{}^T$ did not prove to be significant against total body weight, total body weight$^{1/3}$, or any of the segment length measures for a majority of muscles. On average, less than 3 out of 21 muscles showed significance for any given regression.

Muscle morphometry characteristics for elbow and shoulder muscles for *Macaca fascicularis* are listed in Table 5. As for *M. mulatta*, $L_0{}^M$, mass, PCSA, $L_S{}^T$, and α_0 values with standard deviations are given. To compare *M. fascicularis* muscle measures to *M. mulatta*, mean values for muscle mass, PCSA, and fascicle lengths were scaled by total body weight, total body weight$^{2/3}$, and total body weight$^{1/3}$, respectively, and plotted in Figure 8. As most muscles fell on or near the unity line, the larger mean values of muscle parameters between in *M. mulatta* seemed to be related to the larger average mass of the *M. mulatta* specimens.

While muscle parameters scaled well between the two species of monkeys, scaled parameters were consistently lower for humans as compared to *Macaca mulatta*. Wood et al. (1989) measured human muscle mass and PCSA in human arm muscles. Figure 9 illustrates that scaled human muscles measures were less than scaled *M. mulatta* measures. The one exception to this trend is that middle deltoid is proportionally heavier in humans, although its PCSA is still proportionally lower than might be expected based solely on specimen sizes.

Limb Segment Morphometry

Segment mass and inertial properties for *Macaca mulatta* and *M. fascicularis* are displayed in Tables 6 and 7, respectively. Center of mass distances and ρ-values are given as a percentage of segment length. Moments of inertia are given both as mean values from each specimen, and also calculated using the mean value for ρ applied to a hypothetical *M. mulatta* based on average inertial properties recorded in this study. Values for ρ had low standard deviations across different specimens, on average less than 5% of the measured value. ρ also remained fairly constant across different segments, with averages ranging from 24.6% to 26%. The use of ρ to generate mean I_{cg} and I_{prox} values appeared to match measured data quite well, differing on average by under 5%.

Macaca mulatta segment masses and I_{cg} show a relationship with total body weight, as indicated by positive slopes for all segments (Fig. 10a,b). The former shows a significant correlation for upper arm, forearm, and forearm/hand, while the latter shows a significant correlation in upper arm and forearm, as presented in Table 8. Values for these regressions are presented in this table. The term ρ, on the other hand, shows no correlation to total body weight (Fig. 10c).

We have two methods for estimating a segment's moment of inertia. First, we can apply the linear regression for I_{cg} against total body weight in Table 8 to the total body weight of the animal. Second, we

TABLE 6. Macaca mulatta; *mean segment morphometry data (n = 6)*

	Upper arm	Forearm	Hand
Segment mass (g)	294 ± 119	194 ± 78	57 ± 11
Segment mass (% of total body weight)	3.8 ± 0.7	2.5 ± 0.4	0.8 ± 0.3
Segment center of mass (% of segment length)	50 ± 3	44 ± 2	39 ± 2
Radius of gyration ρ (% of segment length)	24.7 ± 1.6	26.0 ± 0.8	24.8 ± 0.9
I_{prox} mean value ($g \cdot cm^2$)	1.63E + 04 ± 5.64E + 03	1.07E + 04 ± 6.36E + 03	1.35E + 03 ± 5.31E + 02
I_{prox} calculated from ρ ($g \cdot cm^2$)	1.66E + 04	1.01E + 04	1.32E + 03
I_{cg} mean value ($g \cdot cm^2$)	3.24E + 03 ± 1.20E + 03	2.71E + 03 ± 1.46E + 03	3.93E + 02 ± 1.73E + 02
I_{cg} calculated from ρ ($g \cdot cm^2$)	3.27E + 03	2.61E + 03	3.81E + 02

Radius of gyration (ρ) and distance of center of gravity from proximal joint center are percentages of segment length. Moments of inertia are presented ($g \cdot cm^2$) about proximal joint center (I_{prox}) and about center of gravity (I_{cg}). Inertia data are presented as calculated for each monkey individually and averaged (mean value) and also calculated from the average ρ using average segment lengths and masses (calculated from ρ).

can use the mean radius of gyration, which is scaled by segment length (see Eq. 7). This requires the segment mass linear regression in Table 8. Figure 11 compares the actual I_{cg} for the six monkeys in this study to the predicted values using these techniques. The linear regression model provided a better estimate of the moment of inertia of the upper arm, as indicated by the smaller root-mean-square error in Figure 10a. However, for other segments ρ provided a more accurate estimate of moment of inertia.

DISCUSSION

The purpose of this study was to quantify the morphometry of the forelimb of the rhesus monkey, including muscle specific parameters and segment inertial properties. Several additional points were also illustrated. First, while *Macaca mulatta* and *M. fascicularis* appear to have similar muscle parameters when scaled appropriately, human arm muscles were relatively lighter and had reduced cross-sectional areas. Second, while muscle mass and PCSA regressions against total body weight proved significant, other measures did not scale as well. Third, radius of gyration tended to be more accurate for scaling inertial properties of segments as compared to simple regression against body weight.

Accuracy of Rhesus Monkey Model

The extensive use of monkeys such as *Macaca mulatta* and *M. fascicularis* in reaching tasks for motor control research is predicated on the assumption that a monkey forelimb is a good correlate of the human arm. While the present data lacks measures

TABLE 7. Macaca fascicularis; *mean segment morphometry data (n = 6)*

	Upper arm	Forearm	Hand
Segment mass (g)	168 ± 39	124 ± 29	40 ± 18
Segment mass (% of total body weight)	2.9 ± 0.1	2.2 ± 0.2	0.7 ± 0.2
Segment center of mass (% of segment length)	51 ± 4	43 ± 3	38 ± 2
Radius of gyration ρ (% of segment length)	24.5 ± 0.6	25.7 ± 0.6	25.0 ± 0.6
I_{prox} mean value ($g \cdot cm^2$)	7.00E + 03 ± 2.34E + 03	4.75E + 03 ± 7.27E + 02	5.58E + 02 ± 2.37E + 02
I_{prox} calculated from ρ ($g \cdot cm^2$)	7.82E + 03	4.32E + 03	8.30E + 02
I_{cg} mean value ($g \cdot cm^2$)	1.44E + 03 ± 3.70E + 02	1.10 + E03 ± 5.65E + 01	1.86E + 02 ± 1.11E + 02
I_{cg} calculated from ρ ($g \cdot cm^2$)	1.44E + 03	1.13E + 03	4.15E + 02

Radius of gyration (ρ) and distance of center of gravity from proximal joint center are percentages of segment length. Moments of inertia are presented ($g \cdot cm^2$) about proximal joint center (I_{prox}) and about center of gravity (I_{cg}). Inertia data are presented as calculated for each monkey individually and averaged (mean value) and also calculated from the average ρ using average segment lengths and masses (calculated from ρ).

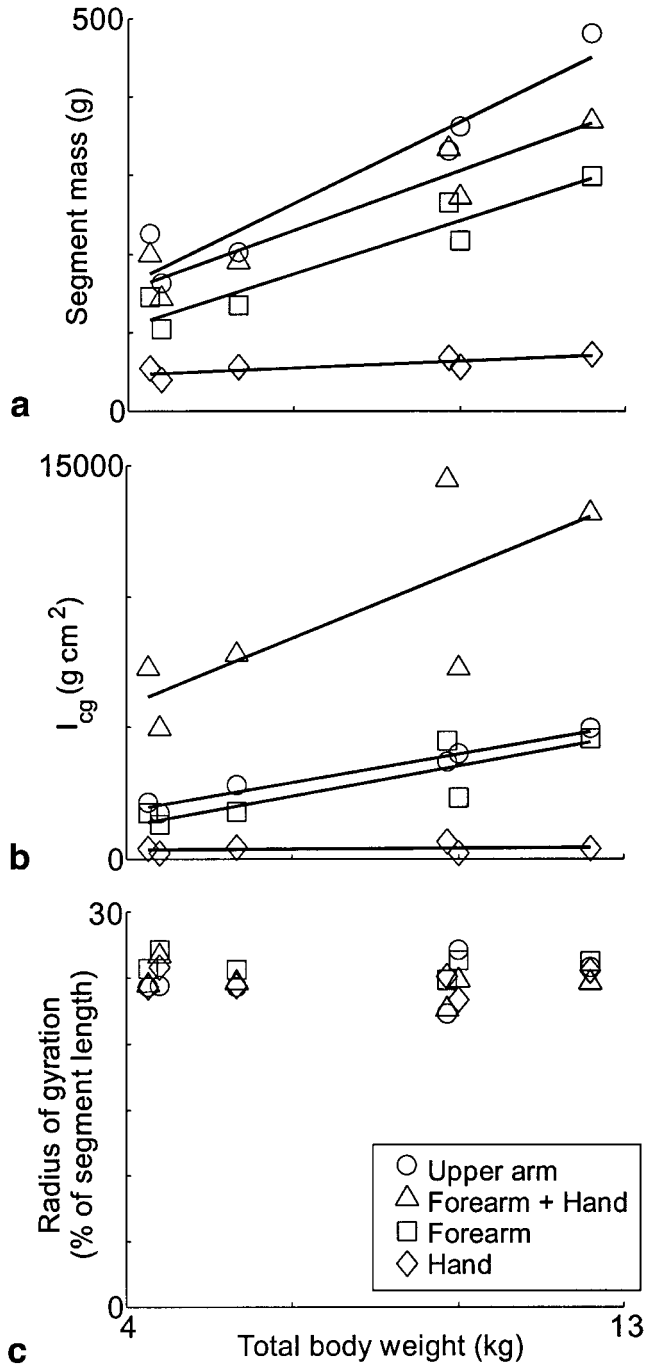

Fig. 10. Comparison of techniques to represent *Macaca mulatta* segment inertia data. **a**: Plot of linear fit of segment mass (g) vs. total body weight (kg). **b**: Plot of measured I_{cg} from each *M. mulatta* specimen (g · cm^2) total body weight (kg). **c**: Plot of calculated radius of gyration (% segment length) against total body weight (kg). In each figure, different icons represent different limb segments (○ = upper arm, △ = forearm + hand, □ = forearm, ◇ = hand).

of moment arm necessary for predicting joint torque, there are several observations on the differences and similarities of limb morphometry that are worth noting.

While muscle properties of *Macaca mulatta* and *M. fascicularis* were quite similar, human muscles were significantly lighter and weaker than would be expected based solely on body mass (Fig. 9). The cumulative PCSA for muscles spanning shoulder and elbow joints in humans was found to lie between 50 and 97 cm^2 on average (Lehmkuhl and Smith, 1983; Wood et al., 1989). Our own data indicates a cumulative PCSA of 57 cm^2 in *M. fascicularis* and 73 cm^2 in *M. mulatta*. At first glance, the human arm seems similar in force producing capability to both species of monkey, but human subject masses were between 10 and 15 times that of monkey. When data are scaled by total body weight$^{2/3}$, PCSA is almost eight times greater in monkeys than in humans. This trend parallels that observed in comparing neck muscles between *M. mulatta* and humans (Richmond et al., 1998). The proportionally greater strength of both monkey species compared to humans may be important when determining equivalent experimental loads and perturbations.

While cross-sectional areas differ between monkeys and humans, the distribution of muscle PCSA between extensors and flexors is more concordant. As a descriptor of limb function, it is expected that muscles that are continually active in a weight-bearing role would have greater cross-sectional areas (i.e., leg muscles in humans, Wickiewicz et al., 1983). Roy et al. (1984) found a ratio of 0.62 using four flexor muscles compared to three extensors in *Macaca fascicularis*. We observed similar values for the same muscles when the cosine of the pennation angle was included. The mean extensor/flexor ratios we observed of 0.58 in *M. fascicularis* and 0.60 in *M. mulatta* correspond closely to the value cited for humans (0.63, Roy et al., 1984). The agreement between monkey and human data are surprising when considering that both species of *Macaca* use their forelimbs for quadrupedal locomotion for a significant amount of time (Napier, 1967). Possibly, forelimb flexors are equivalently hypertrophied by their use during brachiation.

Despite similarities between *Macaca mulatta* and *M. fascicularis*, their forelimb segment proportions differ. *M. fascicularis* had a significantly higher brachial index (forearm length divided by upper arm length as a percentage) compared to *M. mulatta*, with an index of 121%, compared to 108% in *M. mulatta* ($P < 0.05$). In humans, this value is even lower, at 78% (Veeger et al., 1997). Thus, *M. mulatta* may be better suited in these cases as a human arm model. Functionally, it has been suggested that active arboreal quadrupeds have a greater brachial index than do slow-climbing quadrupeds (Walker, 1974). Our measures would suggest that *M. fascicularis* are more like the former category, compared to *M. mulatta*. This hypothesis is supported by the fact that *M. fascicularis* are generally lighter and have much longer, semi-prehensile tails (Hill, 1954); both

TABLE 8. Macaca mulatta; *linear regression from* M. mulatta *data for segment mass (g), I_{cg} (g · cm^2), and ρ (% of segment length) against total body weight (kg)*

		Upper arm	Forearm	Hand	Forearm + Hand
Segment mass	m (g/kg)	34.4	22.4	2.77	25.2
	b (g)	23.0	17.5	35.4	53.0
	P	*	*		*
I_{cg}	m (g · cm^2/kg)	356.6	378.1	11.6	861.6
	b (g · cm^2)	432	−264	301	2381
	P	*	*		
ρ	m (% segment/kg)	0.156	−0.0469	−0.0042	−0.181
	b (% segment)	23.5	26.3	24.8	26.1
	P				

Values for m (slope) and b (Y-intercept) are given. Significance is indicated by an asterisk (*) in the *P* column.

are important factors in facilitating a greater degree of arborealism.

Scaling of Data by Regression

Biomechanical models for a given subject are best constructed using morphometric data measured directly from that subject, but this is not always practical. Rather, EMG, kinematic, and other behavioral and neural data from awake, behaving subjects are typically combined with parameters for musculoskeletal features taken from existing literature. In the case of non-human primates, morphometric data could be collected from each individual specimen after the behavioral data have been collected. However, collection of such data can take a considerable amount of time on each specimen and may not even be feasible. Behavioral and neural data recorded in these juvenile and early adult monkeys occur over many months or years; the mass and overall size of these monkeys may double during the course of the experiment. How, then, should the morphometric parameters of the body be estimated for each animal or human subject?

One general method is to measure the desired parameters from a cadaver with a height and weight similar to that of the subject to be examined, and assume that muscle and segment measures will be similar (e.g., Alexander and Vernon, 1975). In the case of *Macaca mulatta*, this method is not possible because so little published data is available. Even if such values are available, the cadavers may be older than the target subject group or have experienced pathologies that can lead to different body proportions even when matched for total body weight (Malina, 1969). Further, in the absence of any pathology weight increases with age are not distributed evenly among the various body compartments of skin, muscle, and bone (Grand, 1977). Alternately, a method of estimating parameters based on other measures easily obtained in the subject being studied is useful, and regressions are one such method.

For *Macaca mulatta*, muscle mass scaled well with total body weight, while PCSA did to a lesser extent. This is useful for biomechanical models, as the force-producing capability of a muscle can be predicted from total body weight, using the regression for PCSA. On the other hand, we were surprised that regressions for L_0^M, L_S^T, and for the sum of these two measures were not significant with any of the length or total body weight measures, when other studies have had success in scaling musculotendon path lengths between different sized subjects (Hogfors et al., 1987; White et al., 1989). These studies scaled musculotendon path lengths by length, width, and depth measurements for the bones at the origins and insertions of each muscle. This technique was not used in our study, as our dataset was too small to allow regressions using so many independent variables; further, musculotendon path lengths do not correspond with actual fascicle lengths. There have been no previous attempts to scale L_0^M and L_S^T values in primates to account for size effects. However, coefficients of variation for these two measures are low, at 17% and 27%, respectively. This suggests that using mean values for these data appears to be adequate.

Segment Moment of Inertia

One method for estimating a segment's moment of inertia is using a linear regression model based on total body weight (e.g., Vilensky, 1978). For the present data, regressions based on body weight were able to predict the moment of inertia for the upper arm and the forearm, but were less effective in predicting this variable for the hand and the combined properties of forearm and hand (Table 7, Fig. 11). The hand does not scale with total body weight, unlike the upper arm and forearm masses (Table 7). Thus, it follows that for such segments a scaling method accounting only for total body weight may not be effective (e.g., Vilensky, 1978).

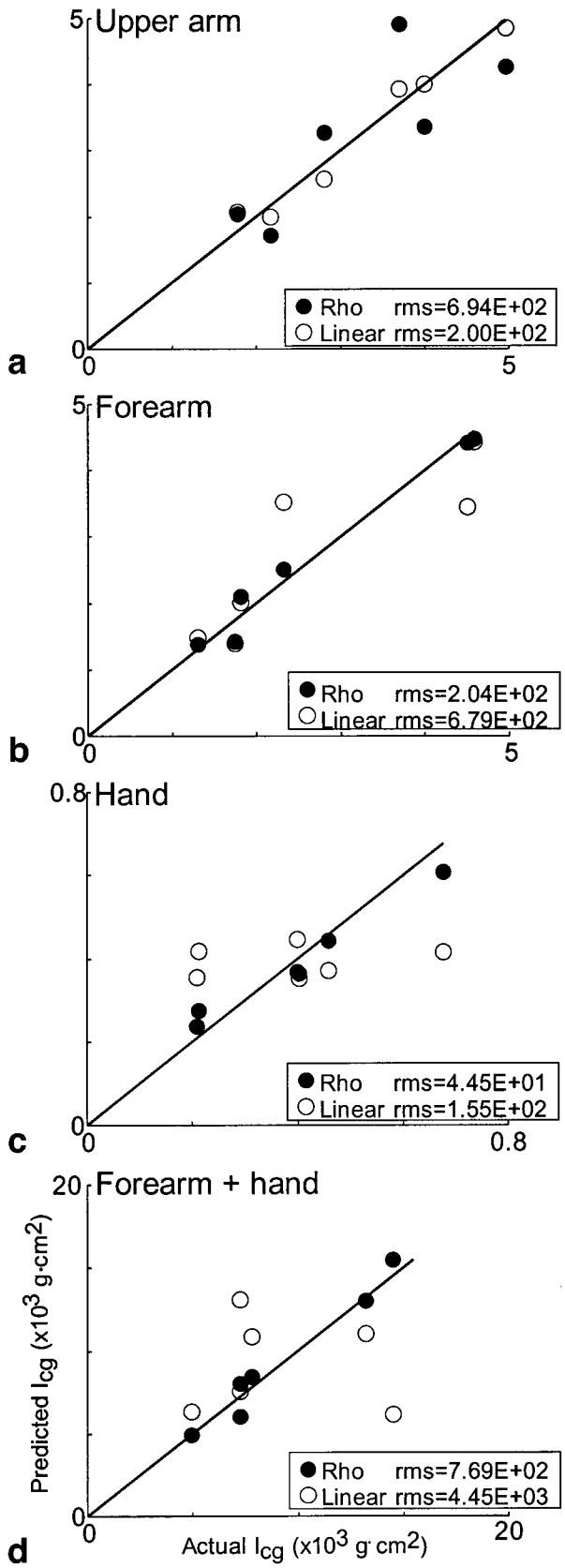

Fig. 11. Comparison of predicted I_{cg} vs. actual measured I_{cg} in various segments for *Macaca mulatta*. I_{cg} was predicted in two ways: by applying the mean radius of gyration (ρ) to segment for each monkey (●), or by applying linear regression against total body weight (○). Segments examined were (**a**) the upper arm, (**b**) forearm, (**c**) hand, and (**d**) the combined forearm and hand. Inset: root-mean-square error for both prediction methods.

As an alternative, we chose to use radius of gyration (ρ) normalized by segment length to scale moment of inertia (e.g., Jensen, 1986). The mean radius of gyration is multiplied by segment length measured from the subject, and then squared and multiplied by segment mass to provide I_{cg}. Segment mass can be determined by the regressions given in Table 7. This provided a segment-specific term for the regression that could be obtained noninvasively. We found that ρ values had low standard deviation and removed any correlation with size (Table 7, Fig. 11c), which suggested the effectiveness of ρ in scaling data from different sized animals (Albrecht et al., 1993).

Muscle Morphometry and Function

It is important to obtain accurate measures of fascicle length, since mathematical models of muscle contraction are dependent on them. Shortening velocity of a muscle is proportional to the number of sarcomeres in series, i.e., fascicle length (Zajac, 1989), while physiological cross-sectional area is most accurately obtained by dividing muscle volume by fascicle length (Gans and Bock, 1965). Using whole muscle length alone, such as in Dornay et al. (1993), is insufficient, as this measure may not correspond with fascicle length, as exemplified by the middle deltoid and the brachialis muscles. Due to the predominant preference for measuring musculotendon path lengths, it is difficult to find fascicle length measures in otherwise extensive morphometry research data (e.g., Wood et al., 1989; Veeger et al., 1997). Even the nomenclature appears to reflect an emphasis on the total musculotendon path length, rather than fascicle length. For example, fascicle length measurements in the present study in monkeys and existing studies in humans (Wood et al., 1989; Veeger et al., 1997) reveal that biceps short head had on average longer fascicles than long head, while triceps lateral head and medial head specimens had longer fascicle lengths than triceps long head.

The intuitive assumption that heavier muscles are able to produce greater force proved false for many monkey forelimb muscles, since PCSA dictates maximal force production, and PCSA is dependent not only on mass but also on fascicle length. Most strikingly, the subscapularis utilizes a complex network of internal tendons to increase its cross-

sectional area such that it is the strongest proximal arm muscle, even compared with much heavier muscles such as pectoralis major and latissimus dorsi. These important muscle parameters cannot be discerned without thorough anatomical study.

ACKNOWLEDGMENTS

The authors thank Dr. G.E. Loeb and F.J.R. Richmond for helpful comments on the manuscript and the members of the Department of Physiology at the University of Montreal for providing many of the cadaveric specimens used in the present study. We also thank J. Creasy and K. Moore for technical assistance.

LITERATURE CITED

Albrecht GH, Gelvin BR, Hartman SE. 1993. Ratios as a size adjustment in morphometrics. Am J Phys Anthropol 91:441–468.

Alexander RMcN, Vernon A. 1975. The dimensions of knee and ankle muscles and the forces they exert. J Hum Mov Stud 1:115–123.

Bodine SC, Roy RR, Meadows DA, Zernicke RF, Sacks RD, Fournier M, Edgerton VR. 1982. Architectural, histochemical, and contractile characteristics of a unique biarticular muscle: the cat semitendinosus. J Neurophysiol 48:192–201.

Caminiti R, Johnson PB, Urbano A. 1990. Making arm movements in different parts of space: dynamic aspects in the primate motor cortex. J Neurosci 10:2039–2058.

Cutts A. 1988. Shrinkage of muscle fibres during the fixation of cadaveric tissue. J Anat 160:75–78.

Dhall U, Singh I. 1977. Anatomical evidence of one-sided forelimb dominance in the rhesus monkey. Anat Anz 141:420–425.

Dornay M, Mussa-Ivaldi FA, McIntyre J, Bizzi E. 1993. Stability constraints for the distributed control of motor behavior. Neural Netw 6:1045–1059.

Doyle WJ, Siegel MI, Kimes KR. 1980. Scapular correlates of muscle morphology in *Macaca mulatta*. Acta Anat 106:493–501.

Forwood MR, Neal RJ, Wilson BD. 1985. Scaling segmental moments of inertia for individual segments. J Biomech 18:755–761.

Fromm C. 1983. Changes of steady state activity in motor cortex consistent with the length-tension relation of muscle. Pflugers Arch 398:318–323.

Gans C, Bock WJ. 1965. The functional significance of muscle architecture—a theoretical analysis. Engeb Anat Entwickl Gesch 38:115–142.

Georgopoulos AP. 1995. Current issues in directional motor control. Trends Neurosci 18:506–510.

Gordon AM, Huxley AF, Julian FJ. 1966. Tension development in highly stretched muscle fibers. J Physiol (Lond.) 184:142–169.

Grand TI. 1977. Body weight: its relation to tissue composition, segment distribution and motor function. J Phys Anthropol 47:241–248.

Hill AV. 1938. The heat of shortening and the dynamic constants of muscle. Proc R Soc Lond B Biol Sci 126:136.

Hill WCO. 1954. Primates: comparative anatomy and taxonomy. VII. Cynopitecinae, eercocebus, macaca, cynopitheca. New York: John Wiley & Sons. p 476–582.

Hogfors C, Sigholm G, Herberts P. 1987. Biomechanical model of the human shoulder. I. Elements. J Biomech 20:157–166.

Hollerbach MJ, Flash T. 1982. Dynamic interactions between limb segments during planar arm movement. Biol Cybern 44: 67–77.

Howell AB, Straus WL Jr. 1961. The muscular system. In: Hartman CG, editor. Anatomy of the rhesus monkey. New York: Hafner. p 89–175.

Hoy MG, Zernicke RF. 1986. The role of intersegmental dynamics during rapid limb oscillations. J Biomech 19:867–877.

Hoy MG, Zajac FE, Gordon ME. 1990. A musculoskeletal model of the human lower extremity: the effect of muscle, tendon and moment arm on the moment-angle relationship of musculotendon actuators at the hip, knee, and ankle. J Biomech 23:157–169.

Jensen RK. 1986. Body segment mass, radius and radius of gyration proportions of children. J Biomech 19:359–368.

Kalaska JF, Cohen DAD, Hyde ML, Prud'homme M. 1989. A comparison of movement direction-related versus load direction-related activity in primary motor cortex, using a two-dimensional reaching task. J Neurosci 9:2080–2102.

Kamibayashi LK, Richmond FJR. 1998. Morphometry of human neck muscles. Spine 23:1314–1323.

Karst GM, Hasan Z. 1991. Timing and magnitude of electromyographic activity for two-joint arm movements in different directions. J Neurophysiol 66:1594–1604.

Kuo AD, Zajac FE. 1993. Human standing posture: multi-joint movement strategies based on biomechanical constraints. Prog Brain Res 97:349–358.

Lehmkuhl LD, Smith LK. 1983. Brunnstrom's clinical kinesiology. Philadelphia: FA Davis. p 391–401.

Lucas SM, Ruff RL, Binder MD. 1987. Specific tension measurements in single soleus and medial gastrocnemius muscle fibers of the cat. Exp Neurol 95:142–154.

Malina RM. 1969. Quantification of fat, muscle and bone in man. Clin Orthop 65:9–38.

Mendez J, Keys A. 1960. Density and composition of mammalian muscle. Metabolism 9:184–188.

Napier JR. 1967. A handbook of living primates: morphology, ecology and behaviour of nonhuman primates. London: Academic Press. p 456.

Pierrynowski MR, Morrison JB. 1985. Estimating the muscle forces generated in the human lower extremity when walking: a physiological solution. Math Biosci 75:43–68.

Richmond FJR, Singh K, Corneil B. 1998. Morphometric and histochemical differences between primate and feline neck muscles (Abstract). Soc Neurosci Abstr 24:1672.

Roy RR, Bello MA, Powell PL, Simpson DR. 1984. Architectural design and fiber-type distribution of the major elbow flexors and extensors of the monkey (Cynomolgus). Am J Anat 171:285–293.

Schneider K, Zernicke RF. 1992. Mass, center of mass, and moment of inertia estimate for infant limb segments. J Biomech 25:145–148.

Schremmer CN. 1967. Gewichtsanderungen verschiedener Gewebe nach Formalinfixierung. Frankfurter Z Pathol 77:299–304.

Scott SH. 1997. Comparison of onset time and magnitude of activity for proximal arm muscles and motor cortical cells before reaching movements. J Neurophysiol 77:1016–1022.

Scott SH. 1999. Apparatus for measuring and perturbing shoulder and elbow joint positions and torques during reaching. J Neurosci Methods 89:119–127.

Scott SH, Kalaska JF. 1997. Reaching movements with similar hand paths but different arm orientations. I. Activity of individual cells in motor cortex. J Neurophysiol 77:826–853.

Scott SH, Loeb GE. 1995. Mechanical properties of aponeurosis and tendon of the cat soleus muscle during whole-muscle isometric contractions. J Morphol 224:73–86.

Scott SH, Winter DA. 1991a. A comparison of three muscle pennation assumptions and their effect on isometric and isotonic force. J Biomech 24:163–167.

Scott SH, Winter DA. 1991b. Talocrural and talocalcaneal joint kinematics and kinetics during the stance phase of walking. J Biomech 24:743–752.

Scott SH, Engstrom CM, Loeb GE. 1993. Morphometry of human thigh muscles. Determination of fascicle architecture by magnetic resonance imaging. J Anat 182:249–257.

Scott SH, Brown IE, Loeb GE. 1996. Mechanics of feline soleus. I. Effect of fascicle length and velocity on force output. J Musc Res Cell Motil 17:207–219.

Seif-Naraghi AH, Winters JM. 1990. Optimized strategies for scaling goal-directed dynamic limb movements. In: Winters JM, Woo SLY, editors. Multiple muscle systems: biomechanics and movement organization. New York: Springer-Verlag. p 312–334.

Sonntag CF. 1922. On the anatomy of the Drill (*Mandrillus leucophaeus*). Proc Zool Soc Lond 1:429–453.

Spector SA, Gardiner PF, Zernicke RF, Roy RR, Edgerton VR. 1980. Muscle architecture and force-velocity characteristics of cat soleus and medial gastrocnemius: implications for motor control. J Neurophysiol 44:951–960.

Veeger HEJ, Yu B, An K, Rozendal RH. 1997. Parameters for modeling the upper extremity. J Biomech 30:647–652.

Vilensky JA. 1978. Masses, centers-of-gravity, and moments-of-inertia of the body segments of the rhesus monkey (*Macaca mulatta*). Am J Phys Anthropol 50:57–65.

Walker A. 1974. Locomotor adaptations in prosimian primates. In: Jenkins FA Jr, editor. Primate locomotion. New York: Academic Press. p 349–382.

Walker SM, Schrodt GR. 1974. I. Segment lengths and thin filament periods in skeletal muscle fibers of the rhesus monkey and the human. Anat Rec 178:63–82.

White SC, Yack HJ, Winter DA. 1989. A three-dimensional musculoskeletal model for gait analysis. Anatomical variability estimates. J Biomech 22:885–893.

Wickiewicz TL, Roy RR, Powell PL, Edgerton VR. 1983. Muscle architecture of the human lower limb. Clin Orthop 179:275–283.

Winter DA. 1979. Biomechanics of human movement. New York: Wiley. p 202.

Wood JE, Meek SG, Jaconbsen SC. 1989. Quantantiation of human shoulder anatomy for prosthetic arm control. I. Surface modeling. J Biomech 22:273–292.

Zajac FE. 1989. Muscle and tendon: properties, models, scaling and application to biomechanics and motor control. Crit Rev Biomed Eng 17:359–411.

Zajac FE, Gordon ME. 1989. Determining muscle's force and action in multi-articular movement. Exerc Sport Sci Rev 17: 187–230.